Investigating the influence of lithium-ion batteries degradation on the parameters of the electric power storage system

Ramis Bulatov[1*], *Rinat* Nasyrov[1], and *Maxim* Burmeyster[1]

[1]National Research University "MPEI", Electrical Power Systems Department, 111250, Moscow, Russian Federation

Abstract. This article deals with the use of a battery-based energy storage system (ESS) to ensure the required power output of power plants (PP) based on renewable energy sources (RES) integrated into the electric power system (EPS). A model of a lithium-iron-phosphate battery-based ESS has been developed that takes into account the calendar and cyclic degradation of the batteries, and the limitations of the conversion subsystem. The nominal capacity and power of the ESS is proposed to be chosen based on two levels of tolerances: the preset range of RES-based power output and the relative period of deviation from the committed power. When choosing the ESS parameters, the features of its operation, as well as restrictions on the part of the EPS, were taken into account. The developed method was applied to the EPS model including solar power plants (SPP) and wind power plants (WPP). In the end of the article, the obtained results are analyzed and the effect of the ESS operation on its residual capacity and service life is shown.

1 Introduction

Due to the possibility of power consumption and output, electric energy storage systems (ESS) allow for their integration into the electric power system (EPS) of generating facilities using renewable energy sources (RES) in their operations. The total global installed capacity of ESS used for the effective RES integration is about 4.18 GW [1]. The vast majority of projects are based on electrochemical energy storage units (in particular, lithium-ion batteries). According to its 2035 Energy Strategy, Russia should ensure the ESS inclusion in the electric power circulation and the related services provision [2]. The large-scale introduction of ESS in the UES of Russia is hindered by their high cost; therefore, the choice of their parameters is an urgent and important task.

The main parameters of the ESS for solving power flow control problems are the nominal capacity and output power. The scientific and technical publications include articles analyzing methods for choosing the parameters of battery-based ESS in order to solve the problems of RES-based power plants (PPs) integrating in EPS [3-7]. In most methods, the ESS parameters are determined focusing on economic criteria: maximizing the profit from the ESS system and RES-based PPs, minimizing the Levelized Cost of Storage (LCOS),

* Corresponding author: bulatov_rv@inbox.ru

maximizing net present value, etc. Methods for determining the ESS parameters in the publications can be divided into probabilistic, analytical, optimization and hybrid ones [8]. The analysis of the articles showed the absence of a universal methodology for choosing the ESS parameters for integrating RES-based PPs into the EPS. Solving specific problems requires the development of new methods or adaptation of existing ones. Another important assumption in many works is the absence of a degradation model for an electrochemical battery, which can lead to an erroneous choice of the ESS parameters required to achieve the desired effect. Thus, the purpose of this research is to develop a methodology for determining the ESS parameters, taking into account the degradation of the electrochemical battery, the stochastic nature of the power output by RES-based generating sources, the power flow distribution in the grid, the actual load of the grid electrical equipment, and energy losses in the ESS.

2 Model of lithium-ion battery-based ESS

2.1 Simulation of the operation of a lithium-ion battery-based ESS

The main element of the battery-based ESS is the rechargeable battery. The most widely used types of lithium-ion batteries, which are characterized by their choice of cathode material, are currently lithium-iron-phosphate (*LFP*) and lithium-nickel-manganese-cobalt (*NMC*) batteries [1]. The ESS load profile in the tasks of RES-based PP's power control requires the storage unit's daily operation in the charge and discharge mode, where the average duration of cycles can be several hours. When the footprint for the ESS placement is unlimited, the most significant factors in choosing the type of battery are cost, service life, and operational safety. In this case, *LFP* batteries are better than *NMC* batteries. Indeed, analysis of recent application projects and ESS market [1] shows a significant shift towards *LFP* batteries, which are considered by market participants to have higher fire safety, operational advantages, and lower cost. Due to the above, this research focused on the choice of parameters for the ESS based on *LFP* batteries.

When simulating the operation of a battery-based ESS, we must take into account the change in the charge level (1):

$$SOC = E_{BESS}/E_{nom.BESS} \quad (1)$$

where SOC is the state of charge coefficient, E_{BESS} – is the current level of energy stored in the battery, $E_{nom.BESS}$ – is the nominal capacity of the ESS.

When the battery is discharged ($P_{BESS} > 0$) at the time step Δt, the new value of the stored energy at i+1 step is determined based on the energy accumulated at the previous step i (2):

$$E_{\text{BESS},i+1} = E_{\text{BESS},i} - \frac{P_{\text{BESS},i}}{\eta_{\text{BESS}}} \cdot \Delta t - \frac{SD_{\%}}{100} \cdot E_{\text{nom.BESS}} \quad (2)$$

where η_{BESS} – is the efficiency factor of ESS, taking into account losses in *LFP* batteries, in the elements of the conversion subsystem, and in the power transformer; $SD_{\%}$ – is the self-discharge of the battery at the time step Δt , expressed as a percentage of the nominal capacity of the ESS.

When the battery is charged ($P_{BESS} < 0$) the value of the stored energy at step i+1 is determined by (3):

$$E_{\text{BESS},i+1} = E_{\text{BESS},i} - P_{\text{BESS},i} \cdot \eta_{\text{BESS}} \cdot \Delta t - \frac{SD_{\%}}{100} \cdot E_{\text{nom.BESS}} \quad (3)$$

The SOC value at step i+1 will be determined by (1). During battery operation, SOC must be within the acceptable range in order to avoid overcharging or excessive discharging of the battery. When the minimum or maximum SOC is reached, the discharging and charging of the ESS are limited, respectively.

2.2 Degradation simulating of a lithium-iron-phosphate battery-based ESS

When simulating the operation of a storage in the form of a battery, it is also necessary to take into account the calendar and cyclic degradation. It is generally accepted that the calendar degradation is associated with the growth of the surface solid electrolyte interphase (SEI), which protects the anode from decomposition and corrosion, and is mainly formed during the first charge of the battery. Over time, SEI undergoes structural deformation, and its thickness increases. Cyclic degradation is mainly associated with the coating of the anode with a layer of lithium, with the decomposition of the electrolyte, and structural changes in the cathode and anode material. All of the above processes ultimately lead to the loss of active lithium ions and a decrease in the energy intensity of the battery. In this case, the degradation rate depends on temperature, current strength/output, depth of discharge, and state of charge [9,10].

It is customary to determine the total loss of battery capacity by summing up the capacity lost in the process of calendar and cyclic degradation. Calculation of the battery capacity loss is a complex task depending on many factors. Figures 1 and 2 show the results of consideration of LFP battery degradation models for similar operating conditions, which were obtained by different researchers [9-17]. Models analysis shows that the depth of discharge per cycle, the number of cycles, current strength/output, and ambient temperature have the greatest effect on cyclic degradation. For calendar degradation, they are temperature and SOC.

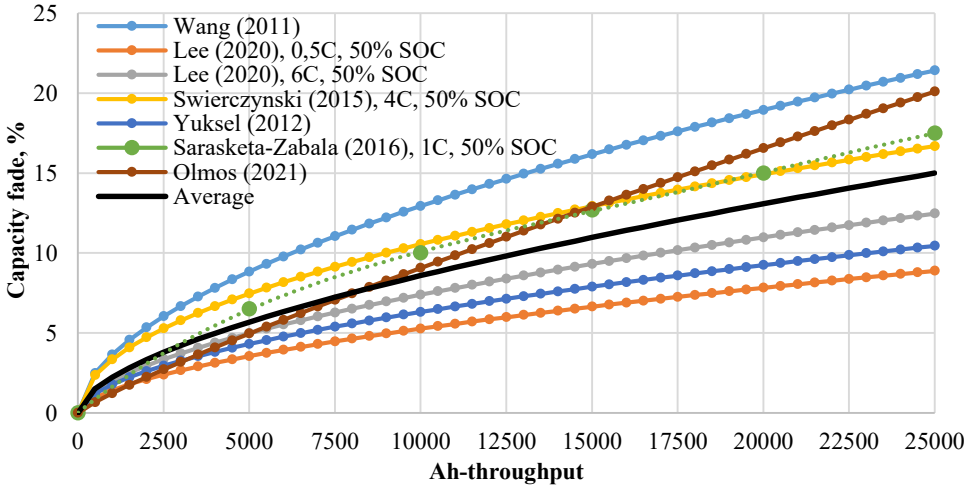

Fig. 1. Capacity loss depending on the charge passed through the battery during cyclic operation.

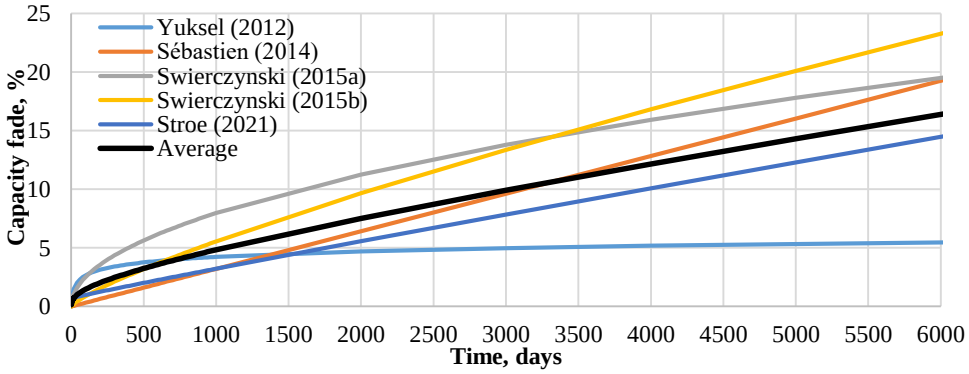

Fig. 2. Capacity loss depending on the time at 25 °C temperature and 50% SOC.

Based on their experiments, some researchers say that for cyclic degradation, the current strength/output factor can be neglected or its effect is minimal [14]. Indeed, the results of the models analysis [11,12] also show that the effect of the current strength manifests itself at the current output starting from 6*C*. To solve the problems of regulating the power flows at RES-based PPs, large values of current output are not required, therefore, this article does not take this factor into account. Since the depth of discharge plays a significant role in battery degradation, this factor can be taken into account by controlling the number of cycles and the depth of discharge at each cycle or by counting the charge that has passed through the battery. Based on the foregoing, the most suitable for solving the problems of this work is the cyclic degradation model from [10], modified as follows (4):

$$\Delta E_{cyc}=7{,}16\cdot10^{-6}\cdot e^{0{,}02717\cdot(T+273{,}15)}\cdot\sqrt{\frac{\frac{P_{BESS}}{\eta_{BESS}}\cdot\Delta t}{2E_{nom.BESS}}} \tag{4}$$

where T_i is ambient temperature, °C.

When deriving expression (4), we assumed that the energy passed through the battery is determined based on the depth of discharge under the condition of returning to the initial state of charge (Full Equivalent Cycle). When determining the expression for cyclic degradation, the experiments were carried out with a current output of 4*C*, which will be a limitation in this work. The calendar degradation model for the same type of battery is taken from [9], which will adequately take into account both degradation processes. Expression for determining calendar degradation is (5):

$$\Delta E_{\text{cal}}=0{,}0025\cdot e^{0{,}1099\cdot T}\cdot e^{0{,}0169\cdot SOC}\cdot t^{\left(-3{,}866\cdot10^{-13}\cdot T^{6{,}635}-4{,}853\cdot10^{-12}\cdot SOC^{5{,}508}+0{,}9595\right)}+0{,}7 \tag{5}$$

where t_i is battery usage time, in days.

2.3 Limitations of the ESS conversion subsystem

The converter imposes a limit on the total output power of the ESS. The ESS converter equipment is often supplied together with a power transformer, so the *PQ* diagram reflects the limitations on power transformer overload. The value of the maximum allowable power factor *cos*φ, as a rule, is 0.9–0.93.

Thus, if it is necessary to produce reactive power in accordance with the control action, it is necessary to check whether relation (6) is satisfied

$$S_{conv}\geq\sqrt[2]{P_{BESS}^2+Q_{BESS}^2} \tag{6}$$

In this case, it is necessary to monitor that the power factor does not exceed the allowable value in accordance with the *PQ* diagram, i. e. (7):

$$\frac{|P_{BESS}|}{\sqrt[2]{P_{BESS}^2+Q_{BESS}^2}}=|cos\varphi|\leq cos\varphi_{max} \tag{7}$$

3 Algorithm for sizing the battery-based ESS parameters

The ESS parameters in this article are determined to solve the problem of maintaining the RES-based PP power output in a given range. It is assumed that every day an operator of a RES-based PP must provide, with the help of ESS, a schedule for providing the committed guaranteed capacity for the day ahead at an hourly interval. The committed power at a certain hour is defined as (8):

$$P_{decl,i}=P_{forecast,i}\pm k\cdot P_{forecast,i}=P_{forecast,i}\pm\Delta P_{max,i} \tag{8}$$

where $i = 1…24$; the k coefficient determines the range of power that will be delivered to the grid.

The ΔP_{max} parameter determines the permissible deviation from the committed power, which can be agreed with the system operator. Thus, the power produced by RES-based PP in the range [$P_{forecast}$ ΔP_{max}, $P_{forecast} + \Delta P_{max}$ is taken as the first level tolerance and can be used as a decision-making parameter in the bidding process on the wholesale power market. As the second level tolerance, we can take the fraction of time $t_{deviation,\%}$, during which the output power of the RES-based PP and ESS P_{comb} do not correspond to the committed power within the first level tolerance. Value $t_{deviation,\%}$ can be taken as an indicator of the reliability of linked ESS and RES-based PPs. Share of time of deviation from the declared power $t_{deviation,\%}$ can be defined as follows (9):

$$t_{deviation,\%} = \frac{1}{N}\sum_{t=1}^{T} P_{*comb,t} \tag{9}$$

where N is the number of time intervals, $P_{*comb,t} = 1$, if $P_{forecast}$ $\Delta P_{max} \le P_{comb,t} \le P_{forecast} + \Delta P_{max}$, $P_{*comb,t} = 0$ in all other cases.

To reduce the required ESS parameters in the implementation of the above approach, the RES initial output power is adjusted using a linear adaptive neuron (ADALINE), the principle of operation of which is described in [18]. Thus, the task is to determine the ESS minimum capacity and power for a fixed k coefficient at various $t_{off,\%}$, taking into account the restrictions imposed by the ESS subsystems and the restrictions on the part of the EPS (no overloads of the grid elements, the required voltage level in the grid nodes, etc.).

4 Simulation and results

The above approach was applied to the model of the grid scheme developed according to the real data and shown in Figure 3. The parameters of overhead lines and loads are shown in Table 1. For WPPs and SPPs, forecast (hourly) and actual (10-minute) power output schedules were obtained in the model. Based thereon, depending on the tolerance value of the first level k and second level $t_{deviation,\%}$, the power and capacity of the ESS were determined.

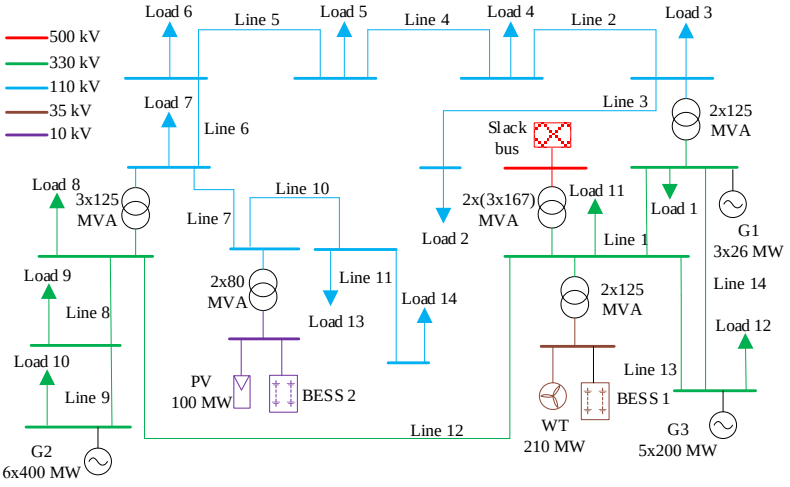

Fig. 3. Fragment of the EPS calculation model.

Steady state conditions for the grid simulated in the *PowerFactory* software package were calculated at 10-minute intervals using the Newton-Raphson method, taking into account the ESS operation. The value of the ESS efficiency is assumed to be 0.9, the value of the

minimum SOC is 10%, the maximum is 90%, the self-discharge of the battery is 0.1% per day. The rated power and capacity of the ESS are related through the current output parameter C_{rate} according to expression (10):

$$P_{nom.BESS} = E_{nom.BESS} \cdot C_{rate} \quad (10)$$

Table 1. Parameters of overhead transmission lines and loads.

No. Line	L, km	r_0, Om/km	x_0, Om/km	$b_0 \cdot 10^{-6}$, Om^{-1}/km	No. Load	Load, MVA
1	10,65	0,048	0,328	3,41	1	339,8+j50,2
2	53,3	0,159	0,413	2,747	2	12+j5,2
3	6,15	0,096	0,429	2,645	3	69,2+j77,9
4	10,9	0,159	0,413	2,747	4	18,2+j7,3
5	2,2	0,244	0,427	2,658	5	13,1+j5,2
6	19,41	0,244	0,427	2,658	6	38,4+j15,3
7	1,54	0,159	0,413	2,747	7	117,6+j24,3
8	83,6	0,0365	0,323	4,64	8	198,1+j0,5
9	6,6	0,0365	0,323	4,64	9	129,6+j51,8
10	21	0,159	0,413	2,747	10	1183+35,7
11	9,3	0,159	0,413	2,747	11	252,3+j30,7
12	74,04	0,096	0,429	2,645	12	59,9+j123
13	12,285	0,0365	0,323	4,64	13	10+j5,4
14	11,45	0,096	0,429	2,645	14	34,5+j14,9

The results of the choice of ESS parameters for SPPs and WPPs are shown in Tables 2 and 3, respectively. For each calculation, the restrictions on the accumulation unit operation were observed, power flows in the branches and voltages in the nodes were also within the allowable range.

Table 2. ESS parameters required to maintain the output power of SPP.

	$t_{deviation,\%} = 5\%$	$t_{deviation,\%} = 10\%$	$t_{deviation,\%} = 15\%$	$t_{deviation,\%} = 20\%$
	$P_{nom.BESS}$, MW/$E_{nom.BESS}$, MW·h			
$k = 0\%$	30/120	25/75	15/45	15/15
$k = 5\%$	27,5/110	20/40	10/10	5/5
$k = 10\%$	25/100	15/30	10/10	5/5
$k = 15\%$	20/60	10/20	5/5	4/2
$k = 20\%$	20/40	5/10	5/1,25	2/0,5

Table 3. ESS parameters required to maintain the output power of WPP.

	$t_{deviation,\%} = 5\%$	$t_{deviation,\%} = 10\%$	$t_{deviation,\%} = 15\%$	$t_{deviation,\%} = 20\%$
	$P_{nom.BESS}$, MW/$E_{nom.BESS}$, MW·h			
$k = 0\%$	40/200	40/160	30/120	35/105
$k = 5\%$	40/200	35/140	25/100	30/90
$k = 10\%$	35/140	30/120	22,5/90	20/80
$k = 15\%$	30/120	30/90	25/75	30/60
$k = 20\%$	35/105	25/75	30/60	25/50

Figures 4 and 6 show power output schedules for RES-based PPs, ESS and declared power output ranges for cases $k = 10\%$ and $t_{deviation,\%} = 10\%$. Figures 5 and 7 show diagrams of the state-of-charge and residual capacity of the ESS. Figure 8 show voltage diagrams at the SPP and WPP connection points. The use of ESS allowed reducing the share of time of deviation from the committed capacity by 8.4 times for WPPs and by 4.7 times for SPPs. The loss of capacity during the operation of ESS amounted to 0.279% of the baseline when working with WPPs, and to 0.270% when working with SPPs. Assuming that the considered modes of RES-based PPs' operation are typical, in 10 years the residual battery capacity will

be 88.845% when working with WPPs, and 88.300% when working with SPPs. The used model of cyclic degradation was obtained at a current output of 4*C*. However, to implement the control action according to the proposed algorithm, ESS is required to work with a current output below 1*C*. In this regard, the obtained values of the loss of ESS capacity turned out to be underestimated. Indeed, in 10 years the residual capacity of the 5 MW and 1.25 MWh ESS (current output 4C), for the case k = 20% and $t_{deviation,\%}$ = 15% (table 2) will be 81.680%.

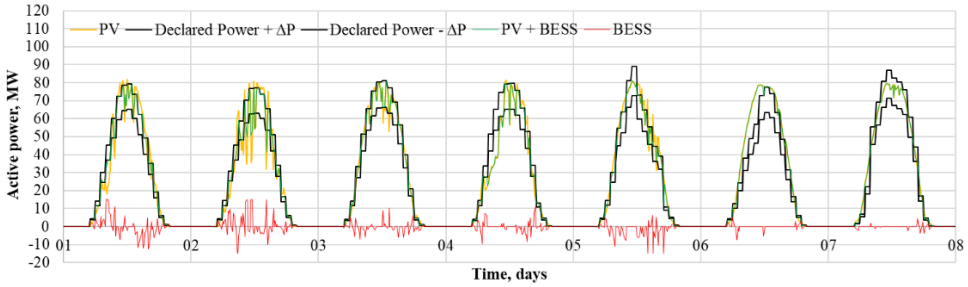

Fig. 4. Diagrams of SPP active power, declared power, and ESS power.

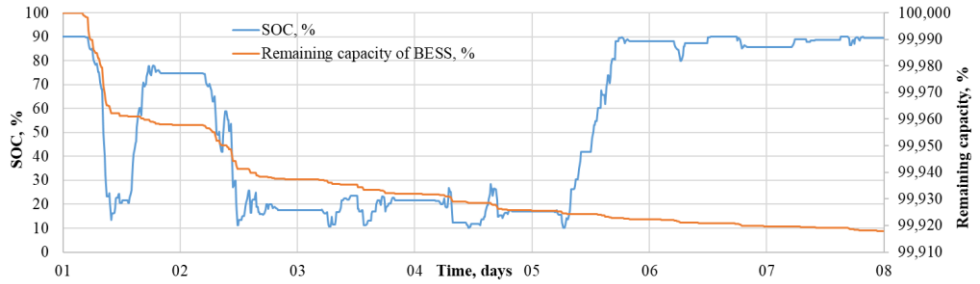

Fig. 5. Diagrams of the dependence of the state of charge and residual energy consumption during the operation of ESS and SPP.

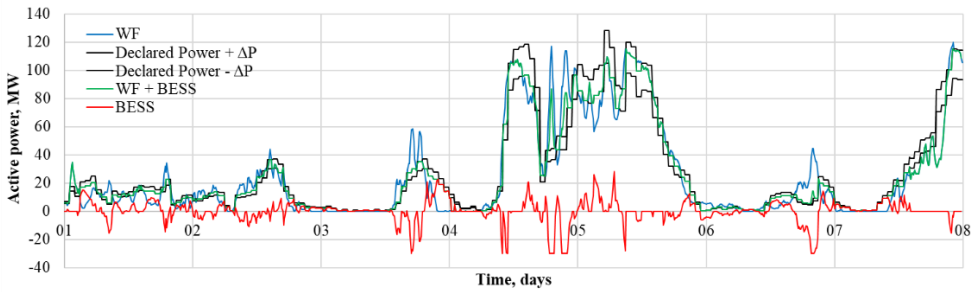

Fig. 6. Diagrams of WPP active power, declared power, and ESS power.

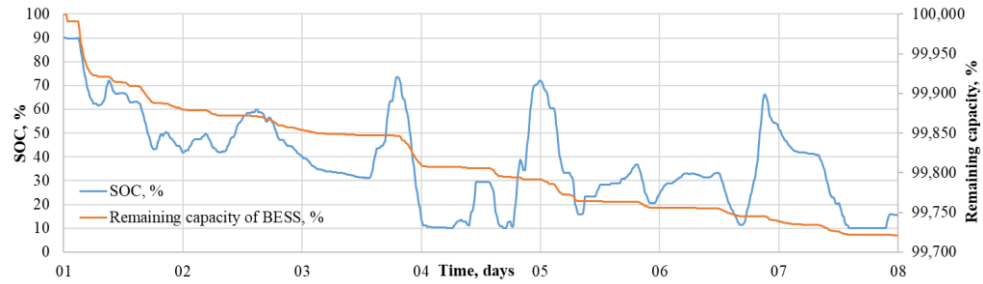

Fig. 7. Diagrams of the dependence of the state of charge and residual energy consumption during the operation of ESS and WPP.

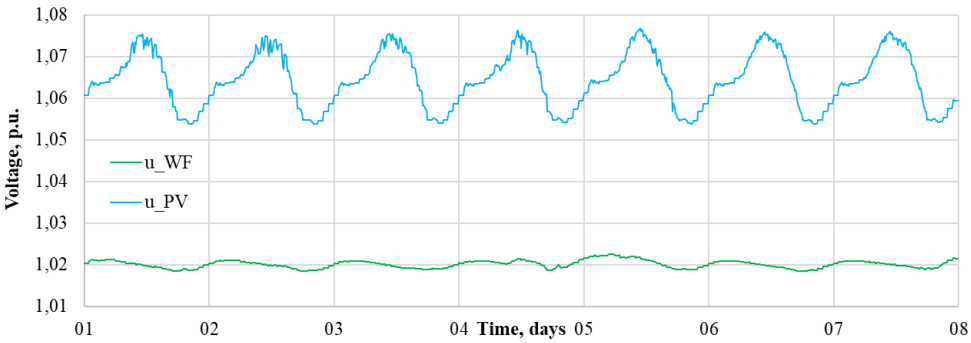

Fig. 8. Diagram of WPP and SPP voltage at the point of connection to the EPS.

The analysis of the obtained results shows that forecasting the power output of WPPs and SPPs is of fundamental importance in determining the ESS parameters. Taking into account the degradation of the lithium-ion ESS allows us to estimate the loss of capacity and the service life of the battery, on the basis of which the ESS' final parameters need to be adjusted.

5 Conclusions

As part of the research, a mathematical model of an ESS based on lithium-iron-phosphate batteries was developed, taking into account the continuous change in the state of charge coefficient, self-discharge of the battery, energy efficiency of the accumulation and conversion subsystems, calendar and cyclic degradation of the batteries, and the limitations of the conversion subsystem and power transformer. A method has been developed that allows determining the power and capacity of the ESS in order to solve the problem of ensuring the output of power from RES-based PPs in a given range based on two tolerance levels: a preset range of power output from RES-based PPs and the relative time of deviation from the committed power. It is shown that the use of ESS allows to effectively control the output power of RES-based PPs, whereas taking into account the battery degradation is necessary for the correct choice of ESS parameters.

The investigation has been carried out within the framework of the project "Development of a prototype virtual inertia system for use in solar and wind power plants as part of a microgrid" with the support of a subvention from the National Research University "MPEI" for implementation of the internal research program "Priority 2030: Future Technologies" in 2022-2024.

References

1. DOE Global Energy Storage Database – URL: https://www.energystorageexchange.org/projects/
2. K.V. Moskvin. *Legal Framework of Electrical Energy Storage Systems.* Energy Law Forum, **3**, 60–65, (2022)
3. V.H. Bui, X.Q. Nguyen, A. Hussain, W. Su. *Optimal Sizing of Energy Storage System for Operation of Wind Farms Considering Grid-Code Constraints*. Energies, **14**, 1-19, (2021)
4. F. Zhang, K. Meng, Z. Xu, Dong Z., L. Zhang, C. Wan, J. Liang. *Battery ESS Planning for Wind Smoothing via Variable-Interval Reference Modulation and Self-Adaptive SOC Control Strategy.* IEEE Transactions on Sustainable Energy, **8(2)**, 695–707, (2017)

5. H. Shin, J. Hur. *Optimal Energy Storage Sizing with Battery Augmentation for Renewable-Plus-Storage Power Plants.* IEEE Access, **8**, 187730-187743, (2020)
6. J. Dulout, B. Jammes, C. Alonso, A. Anvari-Moghaddam, A. Luna, J.M. Guerrero. *Optimal sizing of a lithium battery energy storage system for grid-connected photovoltaic systems.* 2017 IEEE Second International Conference on DC Microgrids (ICDCM), 582-587, (2017)
7. H. Tahir, D.H. Park, S.S. Park, R.Y. Kim. *Optimal ESS size calculation for ramp rate control of grid-connected microgrid based on the selection of accurate representative days.* Int. J. Electr. Power Energy Syst. **139**, (2022)
8. Y. Yang, S. Bremner, C. Menictas, M. Kay. *Battery energy storage system size determination in renewable energy systems: A review.* Renewable and Sustainable Energy Reviews, **91**, 109-125 (2018)
9. X. Sui, M. Swierczynski, R. Teodorescu, D. Stroe. *The Degradation Behavior of LiFePO4/C Batteries during Long-Term Calendar Aging.* Energies, **14** (6), 1-21 (2021)
10. M. Swierczynski, D. -I. Stroe, A. -I. Stan, R. Teodorescu and S. K. Kær. *Lifetime Estimation of the Nanophosphate LiFePO4/C Battery Chemistry Used in Fully Electric Vehicles.* IEEE Transactions on Industry Applications, **51**, 3453-3461 (2015)
11. J. Wang et. al, *Cycle-life model for graphite-LiFePO4 cells.* J. Power Sources, **196**, 3942–3948ϭ (2011)
12. M. Lee, J. Park, S.I. Na, H.S. Choi, B.S. Bu, J. Kim. *An analysis of battery degradation in the integrated energy storage system with solar photovoltaic generation*, Electronics, **9**, No. 4, 1-14 (2020)
13. J. Olmos, I. Gandiaga, A. Saez-de-Ibarra A., X. Larrea, T. Nieva, I.Aizpuru. *Modelling the cycling degradation of Li-ion batteries: Chemistry influenced stress factors*. J. Energy Storage, **40**, pp. 1-17, (2021)
14. E. Sarasketa-Zabala, I. Gandiaga, E. Martinez-Laserna, L.M. Rodriguez-Martinez, I. Villarreal. *Cycle ageing analysis of a LiFePO4/graphite cell with dynamic model validations: Towards realistic lifetime predictions*. Journal of Power Sources, **275**, 573-587ϭ (2015)
15. M. Swierczynski, D. I. Stroe, A. I. Stan, R. Teodorescu. *Lifetime and economic analyses of lithium-ion batteries for balancing wind power forecast error.* Int. J. Energ. Res. **39** (6), 760–770 (2015)
16. T. Yuksel, J. Michalek. *Evaluation of the effects of thermal management on battery life in plug-in hybrid electric vehicles.* Battery Congress (2012)
17. S. Grolleau, A. Delaille, H. Gualous, P. Gyan, R. Revel, J. Bernard, E. Redondo-Iglesias, J. Peter. *Calendar aging of commercial graphite/LiFePO4 cell - Predicting capacity fade under time dependent storage conditions.* Journal of Power Sources, **255**, 450-458 (2014)
18. R. V. Bulatov et. al. *Application of a Battery Energy Storage System to Reduce Fluctuations in the Power Output of a Wind Farm Integrated into the Power System.* Proc. III Intern. Youth Conf. Radio Electronics, Electrical and Power Eng., 1 – 8 (2021)